Scripta Materialia xxx (2015) xxx–xxx

Contents lists available at ScienceDirect

Scripta Materialia

journal homepage: www.elsevier.com/locate/scriptamat

Tunable optical properties of multiphase ZnO–V_2O_5 polycrystalline powders

E. Senthil Kumar [a,b,*], F. Bellarmine [a,1], M. Ramanjaneyulu [a,1], Divya Deepthi [a], M.S. Ramachandra Rao [a,*]

[a] Department of Physics, Nano Functional Materials Technology Centre and Materials Science Research Centre, Indian Institute of Technology Madras, Chennai 600036, India
[b] Department of Materials Science and Engineering, Yonsei University, Seoul 120-749, Republic of Korea

ARTICLE INFO

Article history:
Received 24 April 2015
Revised 19 May 2015
Accepted 19 May 2015
Available online xxxx

Keywords:
Zinc oxide
Optical properties
Zinc vanadate
White emission

ABSTRACT

Bright yellow and white-yellow light emitting ZnO–V_2O_5 polycrystalline powders are synthesized by engineering zinc oxide and different zinc vanadate phases. Emission characteristics strongly depend on different zinc vanadate phases. The bright yellow emission is originated from the $^3T_2 \rightarrow {}^1A_1$ and $^3T_1 \rightarrow {}^1A_1$ transitions in the VO_4 tetrahedra of zinc vanadate phase. White-yellow emission is the combination of blue and green emissions due to native point defects of ZnO and the yellow and red emission from zinc vanadate.

Design and synthesis of ZnO in bulk, thin films and nanostructures form have been of increasing interest due to its excellent optical properties in the near UV and visible region [1–3]. It is well known that non-stoichiometric ZnO exhibits violet, blue and green luminescence due to native point defects, such as zinc interstitials (Zn_i), zinc vacancies (Zn_v) and oxygen vacancies (O_v) respectively [4–8]. The luminescent properties of ZnO can be engineered in various ways like doping, alloying and/or by growing nanostructures with controlled defects [9–11]. For example, Eu doped ZnO nanoparticles showed interesting white light emission [12]. The exciting white emission in this system was attributed to the combined luminescence of ZnO and intra-4*f* transitions of Eu^{3+} ions [13]. Nanostructures of ZnO–Al_2O_3 and ZnO–SiO_2 nanocomposites have shown white light emission and were mainly attributed to the oxygen defects (O_v) at the surface of the ZnO nanostructures [14,15]. Hybrid nanostructures of polyvinyl alcohol/ZnO have also shown white light emission at room temperature [16]. Mordkovich et al. have shown bright luminescent phases in ZnO:W, ZnO:V, ZnO:(W, Mg) and ZnO:(Y, Eu) binary and ternary systems grown by combinatorial pulsed laser deposition methodology [17]. In ZnO–V_2O_5 system, different vanadate phases, viz., ZnV_2O_6, $Zn_2V_2O_7$, $Zn_3V_2O_8$ and $Zn_4V_2O_9$, give fascinating broad band emissions from green to yellow, due to the charge transfer (CT) of an electron from the oxygen 2*p* orbital to the vacant 3*d* orbital of V^{5+} in tetrahedral VO_4 with T_d symmetry [18]. In particular, $Zn_2V_2O_7$ and $Zn_3V_2O_8$ have characteristic crystal structures with dimerized and isolated VO_4 tetrahedra respectively that show interesting luminescent properties [17,18]. Hence it is possible to tune the luminescence characteristics of the zinc vanadate phases by mixing with blue and green emitting ZnO to produce white light emission. We hardly find any report on the luminescent properties of ZnO–V_2O_5 based phosphors in polycrystalline powder form that can be used with blue LEDs for white light emission. Hence in this paper we have made a systematic attempt to develop near UV excitable bright yellow and white-yellow light emitting ZnO–V_2O_5 multiphase system, which can be used for white LEDs applications in near future.

$(1-x)$ ZnO–xV_2O_5 based polycrystalline powders were synthesized using conventional solid-state reaction method. The V_2O_5 mole fraction, *x*, in the polycrystalline samples was varied from 10, 15, 20, 25, 28, 30 to 33 mol% and are denoted as ZV10, ZV15, ZV20, ZV25, ZV28, ZV30 and ZV33 respectively. For example ZV33 represents ZnO–V_2O_5 system with V_2O_5 mole fraction of 0.33. Stoichiometric amounts of ZnO and V_2O_5 were ground thoroughly and heated at 500 °C for 12 h in air in alumina crucibles. Then the powder samples were ground again and heated at 650 °C for 12 h. Presence of different crystalline phases in the as prepared samples was identified by X-ray diffraction (XRD, PANalytical) using Cu K_α radiation (1.5418 Å). Diffuse reflectance spectra (DRS) of the as synthesized powders were measured with Ocean optics (USB 2000) UV–Vis spectrometer using Ba_2SO_4 as a

* Corresponding authors.
E-mail addresses: esenthil5@gmail.com (E. Senthil Kumar), msrrao@iitm.ac.in (M.S. Ramachandra Rao).
[1] Equal contribution.

http://dx.doi.org/10.1016/j.scriptamat.2015.05.042
1359-6462/

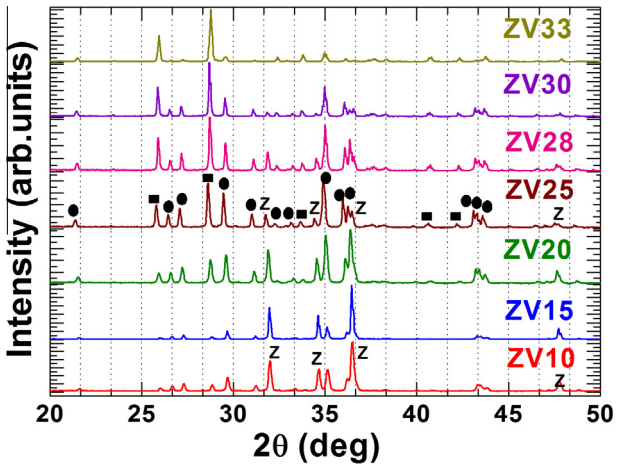

Fig. 1. XRD patterns of ZnO–V_2O_5 polycrystalline powders with V concentration varying from 10 to 33 mol%. Solid squares and circles represent $Zn_2V_2O_7$ and $Zn_3V_2O_8$ phases respectively. ZnO phase is indicated by the letter "*z*".

standard reference. Room temperature photoluminescence (PL) spectra of the samples were recorded using HORIBA JOBIN-YVON (Fluorolog-3-11) spectrofluorometer with xenon lamp (450 W) as the excitation source. The PL spectra were recorded at different excitation wavelengths. Microstructure of the polycrystalline powders were recorded using high resolution scanning electron microscope, (HRSEM: FEI, Quant 400). Chemical compositions of the powder samples were analyzed using energy dispersive X-ray spectrometry (EDS).

Fig. 1 shows XRD patterns of the ZnO–V_2O_5 polycrystalline powder samples with V concentration varying from 10 to 33 mol%. Peaks corresponding to wurtzite ZnO are clearly observed for the samples with V concentration $\leqslant$28 mol%. At lower V concentration, ZnO phase is dominant with three prominent peaks; (100), (002) and (101). As the V concentration increases, intensity of the ZnO phase diminishes and completely disappears for ZV33. Additional reflections corresponding to other phases are also observed in all the samples. A careful analysis of the XRD patterns reveals that the additional peaks belong to different zinc vanadate phases. All the ZnO–V_2O_5 samples show mainly two zinc vanadate phases $Zn_2V_2O_7$ and $Zn_3V_2O_8$. In the XRD spectra, solid squares and solid circles represent $Zn_2V_2O_7$ and $Zn_3V_2O_8$ phases respectively. ZnO phase is represented by the symbol "*z*". The $Zn_2V_2O_7$ crystallizes into monoclinic structure and the $Zn_3V_2O_8$ has orthorhombic crystal structure. The VO_4 tetrahedra in $Zn_2V_2O_7$ are linked through corner oxygen atom forming dimers. On the other hand, the VO_4 tetrahedra are isolated in $Zn_3V_2O_8$ phase [15]. At lower V concentration (<20 mol%), the $Zn_3V_2O_8$ phase dominates along with ZnO and only minor peaks corresponding to $Zn_2V_2O_7$ are visible. However above 28 mol% of V concentration, the presence of ZnO and $Zn_3V_2O_8$ phases are minimal and only $Zn_2V_2O_7$ phase is found to dominate. An interesting observation is that for ZV28 sample, which later showed broad white-yellow luminescence, both the $Zn_2V_2O_7$ and $Zn_3V_2O_8$ phases are dominant.

The HRSEM analysis reveals that the ZnO–V_2O_5 polycrystalline powders exhibit assorted micro and nanostructured morphologies. These structures consist of rods, discs with hexagonal symmetry and some irregular structured particles. Fig. 2(a–e) shows the effect of V concentration on the morphology of the ZnO–V_2O_5 system. Polar nature of ZnO allows the particle to grow along *c*-axis (0001) with a rod like features with a length of 1–2 μm. With increase in V concentration beyond 20 mol%, no hexagonal symmetry is observed in the particles and the samples exhibit only some polyhedral and irregular agglomerated morphology (Fig. 2d and f). This is in agreement with XRD, which showed no detectable hexagonal ZnO phase in the sample ZV33. Composition analysis of different elements like Zn, V and O was carried out using energy dispersive spectroscopy (EDS). All the samples showed reduction in overall V concentration compared to initial value. We found that the Zn/V ratio decreases as the V concentration increases. However, at higher V concentrations ($\geqslant$28%), we have observed more V loss in the samples. Fig. 2f shows the example EDS

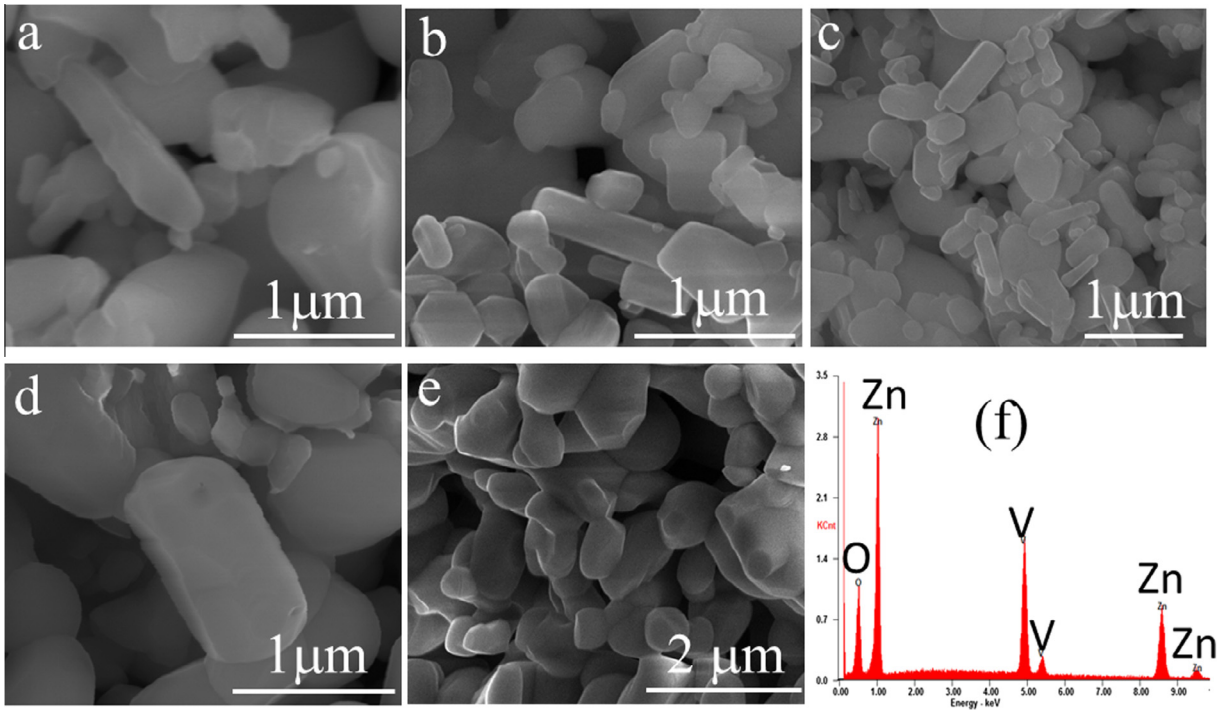

Fig. 2. High-magnification HRSEM images of the ZnO–V_2O_5 powders (a) ZV10, (b) ZV15, (c) ZV20, (d) ZV28 and (e) ZV33. (f) Energy dispersive spectrum of the sample ZV28.